Dalton Transactions

PAPER

View Article Online
View Journal | View Issue

Cite this: *Dalton Trans.*, 2014, **43**, 13070

# Detecting gas molecules *via* atomic magnetization†

Heechae Choi,[a,b] Minho Lee,[b] Seungchul Kim,*[a] Kwang-Ryeol Lee[a] and Yong-Chae Chung*[b]

Received 13th May 2014,
Accepted 2nd July 2014

DOI: 10.1039/c4dt01401d

www.rsc.org/dalton

Adsorptions of gas molecules were found to alter the directions and magnitudes of magnetic moments of transition metal (Co, Fe) atoms adsorbed on graphene. Using first-principles calculations, we demonstrated that magnetism of surface atoms can be used to identify the kind of existing gas molecules *via* spin-reorientation and/or demagnetizations caused by the reconfigurations of 3d electron energy levels of Co and Fe. We suggest for the first time that magnetic properties of transition metal-embedded nanostructures can be used in highly selective gas-sensing applications.

## 1. Introduction

Conventional gas sensors using electrical conductivity distinguish certain kinds of existing gas species by the changes in electric current. In general, electricity-based gas sensors have poor selectivity, causing them to respond to multiple analytes, which is called cross-sensing.[1–4] Especially, toxic gas sensors should be able to exclusively respond to target gas molecules by neglecting atmospheric gases such as $H_2O$, $O_2$, and $N_2$.[1,2] Most of the improvements in the selectivity of toxic gas sensors has been achieved by modifying the device architectures[5] or using new kinds of nanomaterials such as carbon nanotubes and semiconductor nanowires.[2–4] Employing a new kind of property instead of continuously using electric current, despite very few reports being published to date, is said to be the most challenging and innovative way to improve the selectivity of chemical-sensing devices. Even if selectivity on a property is poor when used in gas mixtures, cross-sensitivity does not exist on all properties; thus, the overall sensing result can distinguish target gas species with far better accuracy. In addition, finding a new kind of property to use in gas sensors can broaden the candidate materials and give more possibility of cost-effective device designs.

Spin degree of freedom in devices has provided higher bits of information than binary on/off signals by electric currents.[6–11] Here, we attempt to use electron orbital configurations, which have a higher degree of freedom than electric current, in gas molecule detection. The resultant *signal* represents the magnetic properties of the transition metal (TM) atoms, which are capable of forming chemical bonds with multiple gas species. Our first-principles calculations show that orientations and magnitudes of magnetizations of transition metal atoms on graphene are changed by adsorptions of CO, NO, and $NO_2$ gas molecules by reconfigurations of 3d electron energy levels. The configurations of 3d electron levels induce distinguishable *signals* of CO, NO, and $NO_2$ gas molecules from atmospheric gas species ($H_2O$, $O_2$, $N_2$). The single transition metal atoms (Co, Fe) adsorbed on graphene were chosen for magnetic gas detection in this study for the following reasons: (i) large surface/volume ratio of graphene sheet,[11,12] which is a great advantage for a gas-sensing material, (ii) the stronger adsorptions of toxic gas molecules of our interest (CO, NO, $NO_2$) on metal atoms than on graphene surface,[13–17] and (iii) tunable electron configurations of Co and Fe when being adsorbed on graphene surface so that π-bonds become dominant along the axes of gas molecules, due to the strong π-accepting characteristics of toxic gas molecules, such as CO and NO.[1,2,6,18,19]

Due to the small magnetic anisotropy energies of our suggested structures, the operation temperature is less than few tens of K. However, our first exploration in using magnetism in gas sensing is expected to allow us a wider choice of gas-sensing materials out of pre-existing nanomaterials.

## 2. Calculation method

Density functional theory (DFT) calculations in this study were performed using generalized gradient approximation (GGA) with the projector augmented wave (PAW) pseudopotential

[a]*Center for Computational Science, Korea Institute of Science and Technology, Hwarangro 14 Gil 5, Seoul 136-791, Korea. E-mail: sckim@kist.re.kr*
[b]*Department of Materials Science and Engineering, Hanyang University, 17 Haengdangdong, Seoul 133-791, Korea. E-mail: yongchae@hanyang.ac.kr*
†Electronic supplementary information (ESI) available. See DOI: 10.1039/c4dt01401d

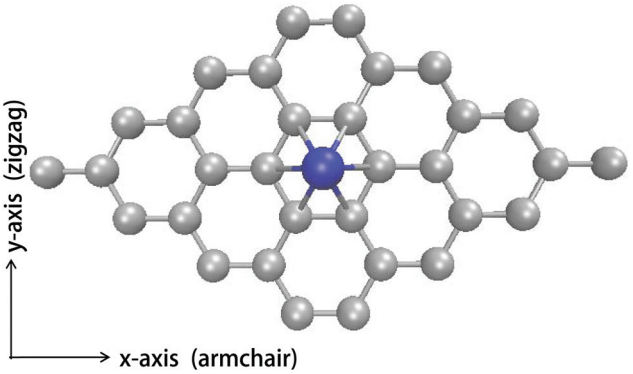


**Fig. 1** Top view of the TM (Co, Fe) adatoms on graphene. The blue and grey spheres are TM adatom and graphene C atoms.

method.[20,21] The PAW method allows to use moderate cut-off energies in the construction of the plane wave basis. All calculations were performed with the Vienna *ab initio* simulation package (VASP)[22,23] using plane wave cut-off energies of 500.0 eV (29.4 Ry). In 4 × 4 graphene supercell, Brillouin-zone integrations were performed using the 4 × 4 × 1 and 14 × 14 × 1 Monkhorst-Pack scheme for structure relaxations and electronic structure calculations, respectively.[24] Positions of atoms were relaxed using the conjugate gradient method until all Hellmann–Feynman forces became smaller than 0.01 eV $Å^{-1}$. The effective range of the cutoff energy and the validity of the mesh density used in our calculations were determined by a convergence test using the theoretically estimated lattice constants of pristine graphene, 2.464 Å. The supercell of the single layer graphene in this study consisted of 32 carbon atoms, and the most stable adsorption site of both Co and Fe atoms was on the center of a hexagonal carbon ring (Fig. 1). The constructed supercells were periodically repeated with a 15 Å vacuum spacer lying along the vertical direction. For the noncollinear magnetism calculations, the spin–orbit coupling (SOC) term was explicitly included. Since SOC is a short-range interaction, a cell with 32 carbon atoms was found to be large enough for a study on spin switching of single TM atoms from our test calculations, which showed differences in magnetic anisotropic energy (MAE) and magnetic moments of Co and Fe less than 10% in magnitude from those on cells with 16 and 24 carbon atoms.

## 3. Results and discussion

Stable atomic structures of gas-adsorbed TM@G were obtained by choosing the lowest energy configuration among several (three to six) trial structures of each gas molecule on each TM@G: placing two opposite directions of vertical alignments, parallel to graphene plane, or in-plane rotation about an axis perpendicular to the graphene. The optimized atomic structures of gas-adsorbed TM@G systems are presented in Fig. 2. The atomic structures of gas-adsorbed Co@G and Fe@G were similar. The $NO_2$ molecule is adsorbed on TM@G with two

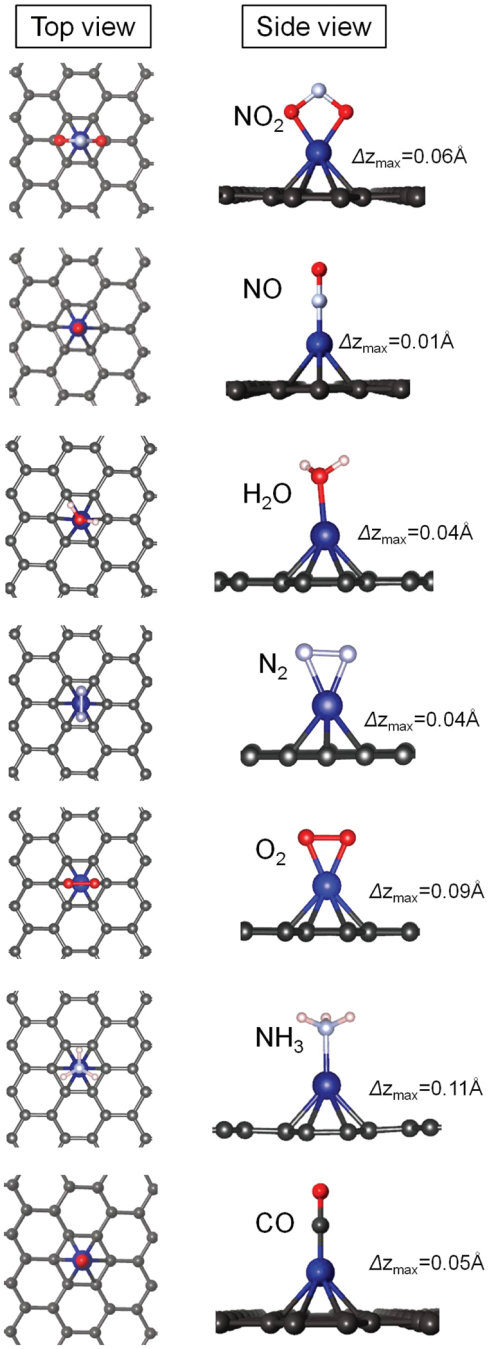


**Fig. 2** Top and side views of gas-adsorbed TM@G systems obtained *via* geometry optimization processes. Dark grey, blue, red, pink, and ice blue sphere indicate C, TM, O, H, and N atoms, respectively. $\Delta z_{max}$ is maximum elevation of carbon atoms in graphene from graphene plane.

oxygen atoms bonded to TM atoms, and O–N–O aligns along the AC direction of graphene lattice. $N_2$ and $O_2$ molecules prefer in-plane alignments along the zigzag (ZZ) and armchair (AC) directions of graphene lattice, respectively. The energy differences between the ZZ- and AC-alignments of $N_2$ and $O_2$ molecules were below 0.05 eV. CO and NO prefer bindings of C and N atoms to TM adatoms in vertical directions with significant amount of energy difference from the opposite direction:

**Table 1** Electron configurations, magnitude of spin magnetic moments ($m_s$), in-plane ($m_L$ (||)) and perpendicular direction ($m_L$ (⊥)) components of magnetic moments and perpendicular magnetic anisotropic energy (PMAE)

| System | Electron configuration | Magnetic moment ($\mu_B$) | $m_L$ (\|\|) | $m_L$ (⊥) | PMAE |
|---|---|---|---|---|---|
| Co@G | $3d^9$ | 1.0 | 0.12 | 1.02 | 0.69 |
| Fe@G | $3d^8$ | 2.1 | 0.13 | 0.05 | −0.90 |

**Table 2** Adsorption energies of gas molecules on graphene-based materials

| | $O_2$ | $H_2O$ | NO | $NO_2$ | CO | $NH_3$ |
|---|---|---|---|---|---|---|
| Pristine graphene [ref. 17] | <0.1 | — | 0.30 | 0.48 | 0.12 | −0.02 |
| B-doped graphene [ref. 27] | 0.01 | 0.04 | 1.07 | 0.33 | 0.02 | 0.02 |
| Functionalized GNR [ref. 28] | 1.88 | — | 2.29 | 2.70 | 1.34 | 0.18 |
| Co/graphene (this work) | 3.63 | 0.80 | 4.41 | 3.15 | 2.46 | 0.98 |
| Fe/graphene (this work) | 3.75 | 0.77 | 3.93 | 3.23 | 2.16 | 1.55 |

0.12 eV for CO on Co@G; 1.86 eV for NO on Co@G; 0.14 eV for CO on Fe@G; 1.73 eV NO on Fe@G. The $H_2O$ molecule prefers O-TM bindings on graphene while O–H arms align along AC direction. The N atom in the $NH_3$ molecule bonds to TM, and N–H bonds align along ZZ direction. TM adsorption little modifies graphene structure. The maximum elevation of carbon atoms ($\Delta z_{max}$) is only 0.11 Å, as it is shown in Fig. 2, and it is much smaller than 0.1 Å for most cases.

We investigated the magnetic properties and electron configurations of Co and Fe atoms on graphene (Co@G and Fe@G) using DFT calculations. As summarized in Table 1, electron configurations of Co and Fe were changed to $3d^9$ and $3d^8$, as the electrons in 4s orbitals of Co and Fe are transferred to the 3d orbitals after being adsorbed on the hollow site of pristine graphene sheet, the most stable adsorption site. The magnetic moment of Co@G ($1.0\mu_B$) is from the unpaired electron in the Co $3d_{yz}$ and $3d_{zx}$ orbitals, whose minority spin states are partially populated above the Fermi level (Fig. 4). Similarly, Fe@G has minority spin states in $3d_{yz}$, and $3d_{zx}$ orbitals populate clearly above the Fermi level, which leads to $2.1\mu_B$ of magnetic moment of Fe adatom. The calculated differential charge isosurface shows that the changed electronic configurations do not originate from the charge transfer between the graphene sheet and the TM adatoms but from the reconfigurations of electrons of TM adatoms (4s to 3d orbitals) (see ESI 1†). The magnetic easy axes of Co@G and Fe@G are in the perpendicular and zigzag (ZZ) directions, respectively, due to the main contributions of the spin–orbit coupling (SOC) term to magnetic anisotropy energy (MAE). The calculated perpendicular magnetic anisotropy energy (PMAE), which is the energy difference between the systems with perpendicular and in-plane magnetizations, of Co@G and Fe@G were 0.69 and −0.90 meV per atom, respectively. The total energy difference of a system with in-plane and perpendicular magnetization, PMAE, was calculated using the equation:

$$\mathrm{PMAE} = E_{\parallel} - E_{\perp},$$

where $E_{\parallel}$ and $E_{\perp}$ are the system total energy with in-plane and perpendicular directions of magnetic moments, respectively. It may be difficult to distinguish atomic spin directions on graphene between armchair and zigzag directions using, for example, spin-polarized scanning tunnel microscopy (SP-STM),[25,26] due to the small in-plane angle difference, 30° in the honeycomb structure. Instead, we assumed that the switching of spin directions of the TM@G from perpendicular to in-plane directions or *vice versa* is a more suitable signal, which can be more easily measured.

The high adsorption energy of a gas molecule on a gas sensor is an important feature for high-speed detection.[27,28] We obtained adsorption energies of gas molecules on TM adatoms, in order to investigate the possibility of TM@G system being used in high-speed sensing compared to conventional graphene or graphene nanoribbon (GNR) sensor systems.[17,27,28] All of the gas species considered in this study bind to TM@G more strongly than on graphene surfaces and functionalized GNR edges. These preferences of gas molecules to adsorb on TM atoms are similar to those in noble metal-embedded graphene systems, as summarized in Table 2. Since gas coverage rate is proportional to adsorption energy, TM@G systems have a capability to uptake gas molecules more quickly than graphene gas sensors, which detect gas molecules *via* electricity.

As the next step, we investigated how electron configurations and magnetizations of TM@G are changed by adsorptions of gas molecules. The calculated PMAE, spin magnetic moments, and adsorption energies of gas molecules, which can be detected using the magnetism of TM@G, are summarized in Table 3. The adsorptions of NO and $NO_2$ on Co@G turns the Co adatom nonmagnetic ($m_s$ = 0) by accepting electrons from Co *via* π-bonds (Fig. 3). As a result, the unpaired electron spin in the highest occupied atomic orbital ($3d_{zx}$ orbital) is transferred to adsorbed gas molecules. On the other hand, adsorptions of $O_2$ and $N_2$ molecules on Co@G switched the spin direction of Co from perpendicular to in-plane direction as $3d_{zx}$ and $3d_{yz}$ electrons in Co@G are transferred to the $2p_z$ orbital of adsorbed $O_2$ and $N_2$ molecules (Fig. 4). When graphene accommodates chemisorptions of gas molecules, such as oxygen or hydrogen, the structures are deformed and the sizeable magnetic moments (up to $1\mu_B$ per atom) are induced, depending on degree of bending or fluctuations.[29,30] However, such atmospheric gas chemisorptions on graphene are hindered by large kinetic energy barriers. Moreover, defect-free graphene is chemically inert; thus, most gas molecules do not react with graphene spontaneously in ambient condition. Therefore, we can expect that the magnetic signals from TM@G are not confused by the chemisorption-induced magnetization of graphene sheet.

As is indicated by the positive PMAE values of Fe@G, the in-plane magnetization of Fe@G is switched to the perpendicular direction when CO and NO are adsorbed.

 

Table 3 Magnetic properties of Co@G and Fe@G with gas molecule adsorptions

| | | $O_2$ | $N_2$ | CO | $NO_2$ | NO | $H_2O$ | $NH_3$ |
|---|---|---|---|---|---|---|---|---|
| Co@G | PMAE (meV per atom) | −0.36 | −1.11 | −0.29 | — | — | 0.64 | 1.05 |
| | $m_s$ | 0.8 | 1.0 | 1.0 | 0 | 0 | 1.0 | 1.1 |
| | $\Delta m_L$ | 0.06 | 0.12 | 0.05 | 0 | 0 | −0.08 | −0.10 |
| Fe@G | PMAE (meV per atom) | −0.20 | 0.25 | 0.38 | −0.36 | 0.60 | −0.14 | −0.26 |
| | $m_s$ | 1.5 | 2.1 | 2.1 | 1.0 | 1.3 | 1.4 | 2.2 |
| | $\Delta m_L$ | 0.04 | −0.02 | −0.05 | 0.02 | −0.05 | 0.02 | 0.03 |

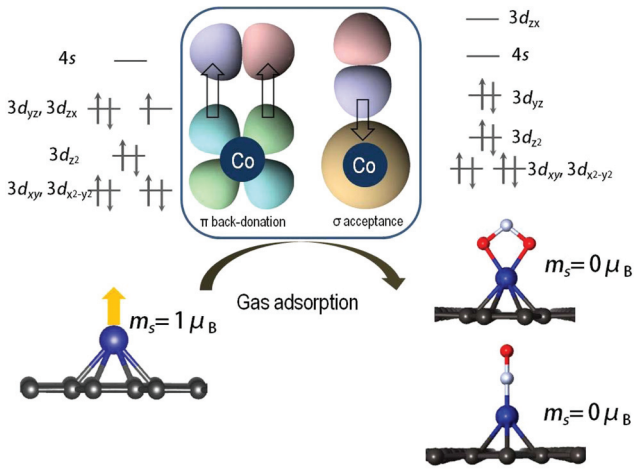


Fig. 3 Schemes of charge transfers between Co@G and NO or $NO_2$ molecule *via* π- and σ-bonding (top) and the electron configurations (middle) and atomic structures (bottom) of Co@G and NO- and $NO_2$-adsorbed Co@G.

Fig. 5 shows the spin switching in Fe@G by the adsorptions of CO and NO and that minority spin states of $3d_{zx}$ and $3d_{yz}$ shift downward below the Fermi level, whereas minority spin states of $3d_{z^2}$ shift above the Fermi level. The Fe@G system, however, does not show changes in magnetization with $O_2$ adsorption. Adsorptions of $NH_3$, $H_2O$, and $CO_2$ molecules on Co@G and Fe@G do not frustrate or rotate the spin moment of Co@G and Fe@G. In other words, three of the target gas molecules (CO, NO, $NO_2$) can be selectively detected even in the existence of atmospheric gas environments ($H_2O$, $O_2$, $N_2$).

The methods to detect of NO, $NO_2$, CO, $O_2$ molecules using the combined signals of Co@G and Fe@G magnetizations are summarized in Table 4. With signals of $m_s$ = 0 in Co@G and the spin reorientations of Fe@G to perpendicular direction, NO and $NO_2$, can be selectively identified. Only CO aligns the spin directions of both Co@G and Fe@G in perpendicular directions, which can be interpreted as the identical signal for the CO molecule. Since the adsorption of $O_2$ or $N_2$ on both Co@G and Fe@G aligns the spin directions to in-plane, the existences of $O_2$ and $N_2$ can also be known.

## 4. Conclusion

Using first-principles calculations, we investigated how the magnetic properties of Co and Fe adatoms on graphene are changed by adsorptions of gas molecules ($O_2$, $H_2O$, NO, $NO_2$, CO, $N_2$, $NH_3$). Measurable changes in the electronic spins of Co@G and Fe@G were found to give distinguishable signals for CO, NO, and $NO_2$ molecules by chemisorptions and resulting reconfigurations of 3d and 4s orbital electrons of Co@G

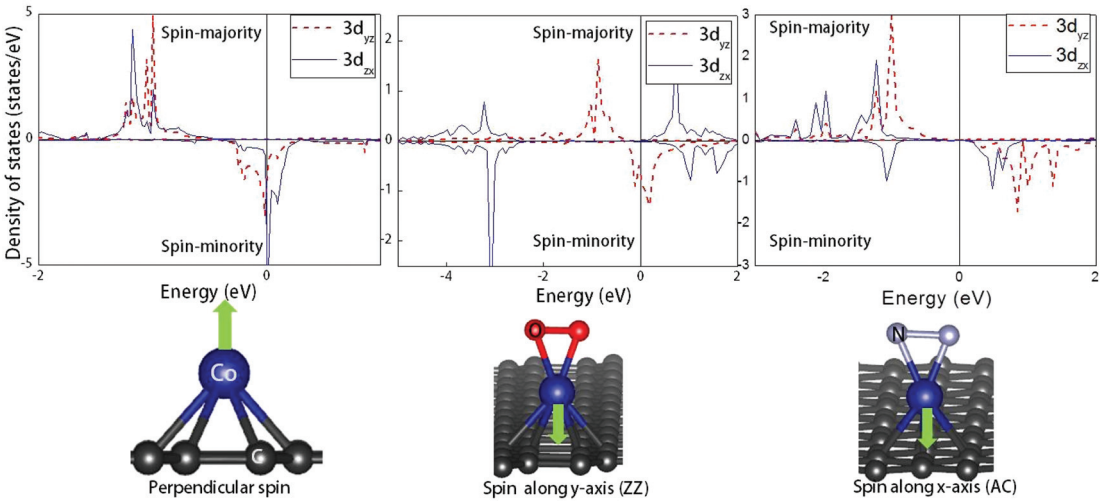


Fig. 4 Atomic structures of $O_2$ and $N_2$ on Co@G and DOS of Co@G before and after adsorptions of $O_2$ and $N_2$.

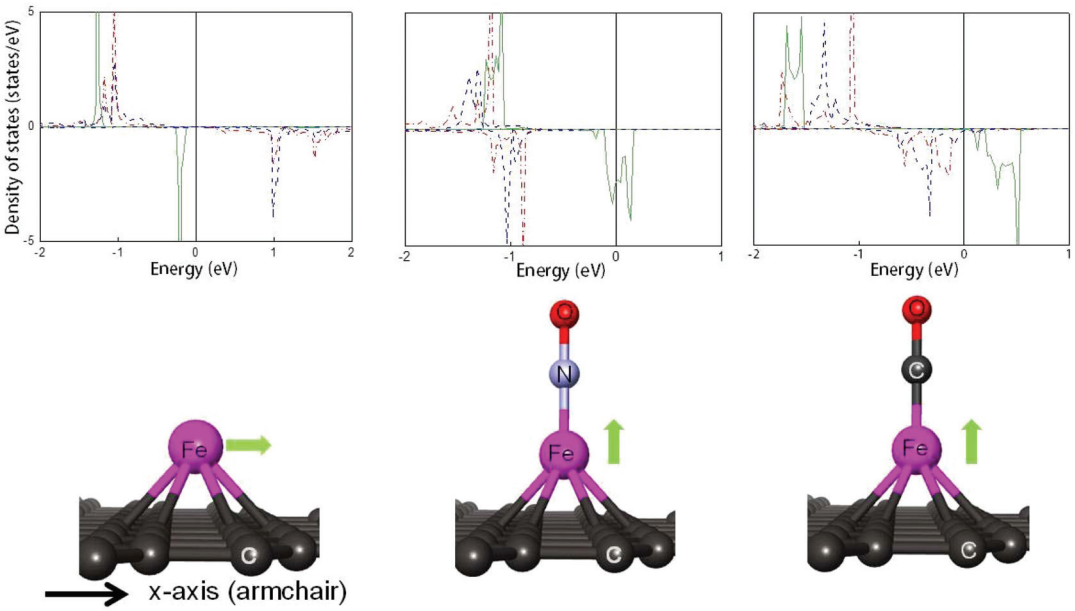


**Fig. 5** Atomic structures and spin directions of Fe@G, and CO- and NO-adsorbed Fe@G (bottom) and corresponding electron density of states of Fe (top).

**Table 4** Detections of NO, $NO_2$, CO, and $O_2$ using changes in magnitude and direction of Co@G and Fe@G

| Co@G | Fe@G | Existing gas |
|---|---|---|
| $m_s = 0$ | Perpendicular | NO |
| $m_s = 0$ | In-plane | $NO_2$ |
| Perpendicular | Perpendicular | CO |
| In-plane | In-plane | $O_2$ or $N_2$ |

and Fe@G. Here, we suggest that gas detection using materials' magnetic properties can make breakthroughs for highly selective and low-power-consuming gas sensor systems due to the higher degree of freedom of 3d orbital electron configuration We expect that similar advanced works with other nanomaterials, such as magnetic semiconductors, oxides[29] or defective carbon structures,[30–34] can overcome such barriers.

## Acknowledgements

H. Choi was supported by the internal project of Institute for Multidisciplinary Convergence of Matter (IMCM) of Korea Institute of Science and Technology (KIST), Exploratory & Creative Research (grant no. 2E23392). S. Kim and K.-R. Lee were supported by the Converging Research Center Program through the Ministry of Science, ICT and Future Planning, Korea (grant no. 2013K000176). M. Lee and Y.-C. Chung were supported by the Basic Science Research Program of National Research Foundation (NRF) of Korea (NRF-2014R1A1A2A10064432).

## References

1 J. F. Boyle and K. A. Jones, The effects of CO, water vapor and surface temperature on the conductivity of a $SnO_2$ gas sensor, *J. Electron. Mater.*, 1977, **6**, 717–733.
2 X. Wang, *et al.*, Batteryless chemical detection with semiconductor nanowire, *Adv. Mater.*, 2011, **23**, 117–121.
3 T. Zhang, S. Mubeen, N. V. Myung and M. A. Deshusses, Recent progress in carbon nanotube-based gas sensor, *Nanotechnology*, 2008, **19**, 332001–332014.
4 F. Schedin, *et al.*, Detection of individual gas molecules adsorbed on graphene, *Nat. Mater.*, 2007, **6**, 652–655.
5 G. Alain, C. H. Shim, M. Philippe, and L. François, Chemoresistor type gas sensor having a multi-storey architecture, *European Patent*, 2 533 037 A1, 2012.
6 M. N. Baibich, J. M. Broto, A. Fert, F. Nguyen Van Dau and F. Petroff, Giant magnetoresistance of (001)Fe/(001)Cr magnetic superlattices, *Phys. Rev. Lett.*, 1988, **61**, 2472–2475.
7 S. M. Wu, *et al.*, Reversible electric control of exchange bias in a multiferroic field-effect device, *Nat. Mater.*, 2010, **9**, 756–761.
8 S. A. Wolf, *et al.*, Spintronics: A spin-based electronics vision for the future, *Science*, 2001, **294**, 1488–1495.
9 P. Gambardella, *et al.*, giant magnetic anisotropy of single cobalt atoms and nanoparticles, *Science*, 2003, **300**, 1130–1133.
10 F. Meier, L. Zhou, J. Wiebe and R. Wiesendanger, Revealing magnetic interactions from single-atom magnetization curve, *Science*, 2008, **320**, 82–86.
11 T. Balashov, *et al.*, Magnetic anisotropy and magnetization dynamics of individual atoms and cluster of Fe and Co on Pt (111), *Phys. Rev. Lett.*, 2009, **102**, 257203–257206.

12 H. Da, Y. P. Feng and G. Liang, Transition-Metal-Atom-Embedded Graphene and Its Spintronic Device Applications, *J. Phys. Chem. C*, 2011, **115**, 22701–22706.
13 K. R. Ratinac, W. Yang, S. P. Ringer and F. Braet, Toward ubiquitous environmental gas sensors-capitalizing on the promise of graphene, *Environ. Sci. Technol.*, 2010, **44**, 1167–1176.
14 Y. H. Zhang, *et al.,* Improving gas sensing properties of graphene by introducing dopants and defects: a first-principles study, *Nanotechnology*, 2009, **20**, 185504–185512.
15 Q. Ji, *et al.,* Layer-by-layer films of graphene and ionic liquids for highly selective gas sensing, *Angew. Chem., Int. Ed.*, 2010, **122**, 9931–9933.
16 Y. Lu, B. R. Goldsmith, N. J. Kybert and A. T. C. Johnson, DNA-decorated graphene chemical sensors, *Appl. Phys. Lett.*, 2010, **97**, 083107–083109.
17 M. Zhou, Y. H. Lu, Y. Q. Cai, C. Zhang and Y. P. Feng, Adsorption of gas molecules on transition metal embedded graphene: a search for high-performance graphene-based catalysts and gas sensors, *Nanotechnology*, 2011, **22**, 385502–385509.
18 J. P. Perdew, *et al.,* Atoms, molecules, solids, and surfaces: Applications of the generalized gradient approximation for exchange and correlation, *Phys. Rev. B: Condens. Matter*, 1992, **46**, 6671.
19 J. P. Perdew, K. Burke and M. Ernzerhof, Generalized gradient approximation made simple, *Phys. Rev. Lett.*, 1996, **77**, 3865–3868.
20 G. Kresse and D. Joubert, From ultrasoft pseudopotentials to the projector augmented-wave method, *Phys. Rev. B: Condens. Matter*, 1999, **59**, 1758–1775.
21 G. Kresse and J. Furthmuller, Efficient iterative schemes for ab initio total-energy calculations using a plane-wave basis set, *Phys. Rev. B: Condens. Matter*, 1996, **54**, 11169–11186.
22 H. J. Monkhorst and J. D. Pack, Special points for Brillouin-zone integrations, *Phys. Rev. B: Condens. Matter*, 1976, **13**, 5188.
23 H. Valencia, A. Gil and G. Frapper, Trends in the adsorption of 3d transition metal atoms onto graphene and nanotube surfaces: a DFT study and molecular orbital analysis, *J. Phys. Chem. C*, 2010, **114**, 14141–14153.
24 S. Tang and Z. Cao, Adsorption of nitrogen oxide on graphene and graphene oxides: insights from density functional calculations, *J. Chem. Phys.*, 2011, **134**, 044710–444724.
25 P. Gambardella, *et al.,* Supramolecular control of the magnetic anisotropy in two-dimensional high-spin Fe arrays at a metal interface, *Nat. Mater.*, 2009, **8**, 189–193.
26 C. F. Hirjinbehedin, *et al.,* Large magnetic anisotropy of a single atomic spin embedded in a surface molecular network, *Science*, 2007, **317**, 1199–1203.
27 J. Dai, J. Yuan and P. Giannozzi, Gas adsorption on graphene doped with B, N, Al, and S: A theoretical study, *Appl. Phys. Lett.*, 2009, **95**, 232105–232107.
28 B. Huang, Z. Li, Z. Liu, G. Zhou, S. Hao, J. Wu, B.-L. Gu and W. Duan, Adsorption of Gas Molecules on Graphene Nanoribbons and Its Implication for Nanoscale Molecule Sensor, *J. Phys. Chem. C*, 2008, **112**, 13442–13446.
29 O. V. Yazyev and L. Helm, Defect-induced magnetism in graphene, *Phys. Rev. B: Condens. Matter*, 2007, **75**, 125408.
30 A. Punnoose, K. M. Reddy, J. Hays, A. Thunber and M. H. Engelhard, Magnetic gas sensing using a dilute magnetic semiconductor, *Appl. Phys. Lett.*, 2006, **89**, 112509.
31 M. Choi, J. Son, H. Choi, H.-J. Shin, S. Lee, S. Kim, S. Lee, S. Kim, K.-R. Lee, S. J. Kim, B. H. Hong, J. Hong and I.-S. Yang, *J. Raman Spectrosc.*, 2014, **45**, 168–172.
32 Ž. Šljivančanin, R. Balog and L. Hornekær, Magnetism in graphene induced by hydrogen adsorbates, *Chem. Phys. Lett.*, 2012, **541**, 70–74.
33 T. Schiros, *et al.*, Connecting Dopant Bond Type with Electronic Structure in N-doped Graphene, *Nano Lett.*, 2012, **12**, 4025–4031.
34 H. Gao, *et al.*, A simple method to synthesize continuous large area nitrogen-doped graphene, *Carbon*, 2012, **50**, 4476–4482.